COMMUNICATION

Vertically standing, highly ordered, and dimension and morphology controllable TiO$_2$ nanotube arrays *via* template-assisted atomic layer deposition†

Lee Kheng Tan,[ab] **Xiaogang Liu**[ab] **and Han Gao**[*a]

We demonstrate that TiO$_2$ nanotube arrays (TNTAs) prepared by template-assisted atomic layer deposition (ALD) has successfully yielded vertically standing, highly ordered, and dimension and morphology controllable TNTAs on substrates. The prepared TNTAs are ideal photoanode structures in solid-state dye sensitized solar cells (DSSCs) for enhanced solar energy conversion efficiency.

Titanium dioxide (TiO$_2$) nanotubes in a vertically aligned orientation is a promising configuration for dye-sensitized solar cells (DSSCs).[1,2] The tubular nanostructure provides a high surface area that enables efficient absorption of dye molecules on both external and internal surfaces. In addition, highly ordered 1D TiO$_2$ nanotube arrays (TNTAs) are known to exhibit a lower charge carrier recombination rate as compared to randomly aligned nanotube structures.[3]

While there are many approaches to synthesize 1D TNTAs, self-organized TNTAs are promising as they can be easily prepared using Ti sheets through an electrochemical anodization process.[2–5] Schmuki and co-workers first reported the dye sensitization of TNTAs fabricated from direct anodization of Ti sheets.[2] However, since the Ti substrate is opaque, there is a loss of the incident solar energy as the illumination is performed through the counter electrode. Other literatures reported on the formation of disordered "nanograss" structures on the top morphology[6,7] or collapsed and bundling of these self-organized nanotubes.[8,9] Till present, there are still various fabrication challenges[10–17] for TNTA-based solar cells, including controlled growth of TNTAs with precise dimensions, near perfect ordered TNTAs on substrates, and morphology controlled growth with an increased surface area. As such, a versatile technique to fabricate TNTAs with orientation arrangement, dimension and morphology variations can be realized by using a porous anodic alumina (PAA) template and atomic layer deposition (ALD) technique.

In this work, we prepare vertically standing, highly ordered, and dimension and morphology controllable TNTAs on ITO glass substrates *via* PAA template-assisted ALD (experimental details in ESI†). We demonstrate TNTAs with near perfect ordered, tunable dimensions and morphology using three different types of PAA templates as shown in Fig. 1. a) Near-perfect ordered PAA template by step and flash imprint lithography (SFIL)-based method.[18] b) Dimension and morphology controlled PAA template by controlled anodization yielding 1D single branched and c) 3D multi-tiered branched template.[19] These templates were conformally deposited and filled layer by layer with TiO$_2$ films at atomic-level control using the ALD technique.[20,21] ALD film growth also provides less grain boundaries which can potentially reduce charge trapping and enhance charge transport as photoanode structures.[22,23] Upon releasing the TNTAs from the template, vertically standing TNTAs that are perpendicularly aligned to the substrates can be prepared by CO$_2$ critical point drying. The drying process by CO$_2$ and ethanol prevents capillary forces that are created during the air drying process. TNTAs from the air drying process can cluster together and also form cracks which can decrease electron transport through the cylindrical morphology to the electron-collecting substrates. These TNTAs are anatase when annealed in air at 400 °C for 1 h (XRD data in ESI†). Finally, we characterize the pore filling of the prepared TNTA-based solid-state dye-sensitized solar cells (DSSCs) using solid-state hole transport materials.[24–26] We have qualitatively and quantitatively compared the infiltration of dye (D102) and hole-conducting material (spiro-OMeTAD) between vertically well-aligned TNTAs and TNTAs that have bundled on the substrates.

TNTAs were prepared by depositing ALD TiO$_2$ onto an anodized Al film on transparent conductive ITO substrates. The TNTAs were released from the PAA template by firstly removing the TiO$_2$ overlayer on top of the template using reactive ion etching, and subsequently removing the whole template by wet chemical etching using 1 M KOH, followed by DI water rinsing and air-drying. During the air drying process where water was removed, capillary forces between the NTs were produced and resulted in the bundling of the NTs. This capillary stress was found to be negligible for low aspect ratio NTs and non-negligible for high aspect ratio NTs. Fig. 2A and 2B show the top and cross-sectional view of TNTAs at a low aspect ratio of 3, with a diameter of 65 nm, height of 200 nm, interpore spacing of

[a]Institute of Materials Research and Engineering, 3 Research Link, Singapore 117602. E-mail: h-gao@imre.a-star.edu.sg; Fax: (+65) 6772 7744; Tel: (+65) 6872 7526
[b]Department of Chemistry, National University of Singapore, Singapore 117543

† Electronic supplementary information (ESI) available: Details of experimental procedures, XRD and EDX data. See DOI: 10.1039/c1jm12239h
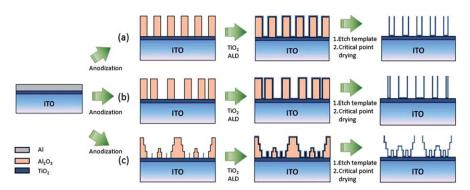
Fig. 1 TNTAs prepared by template-assisted ALD using 3 different types of PAA templates. (a) Near-perfect ordered PAA template from step and flash imprint lithography. (b) Dimension and morphology controlled PAA template by controlled anodization yielding 1D single branched template and (c) 3D multi-tiered branched template.
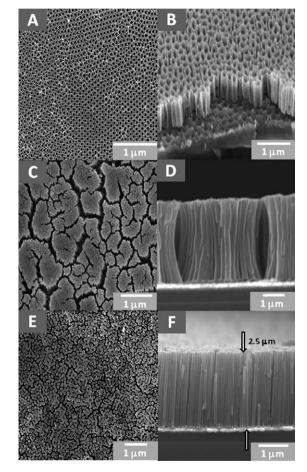

Fig. 2 TNTAs prepared by template-assisted ALD. Top view (A) and cross-sectional view (B) of SEM images show vertically standing TNTAs which are air-dried. The TNTAs have a low aspect ratio of 3, diameter of 65 nm, height of 200 nm, interpore spacing of 110 nm and wall-thickness of 20 nm. Top view (C) and cross-sectional view (D) of SEM images show TNTAs which are air-dried and bundled together. The TNTAs have a high aspect ratio of 30, diameter of 65 nm, height of 2 μm, interpore spacing of 110 nm and wall-thickness of 20 nm. Top view (E) and cross-sectional view (F) of SEM images show vertically standing TNTAs which are dried by a CO_2 critical point dryer. The TNTAs has a high aspect ratio of 30, diameter of 65 nm, height of 2 μm, interpore spacing of 110 nm and wall-thickness of 20 nm.

110 nm and wall-thickness of 20 nm. These TNTAs were air-dried after etching and no bundling or clustering of the NTs was observed. However, air-dried NTs clustered and bundled together at a higher aspect ratio of 30, with a diameter of 65 nm, height of 2 μm, interpore spacing of 110 nm and wall-thickness of 20 nm, as shown in the top and cross-sectional view in Fig. 2C and 2D, respectively. Instead of air drying the TNTAs, we employed a lower surface tension solvent, such as ethanol, and a CO_2 critical point dryer, to dry the TNTAs after template removal. As observed in Fig. 2E and 2F, each of the high aspect ratio NTs stand independently and firmly straight on the ITO substrates after CO_2 critical point drying. This method of drying eliminates the formation of bundling in TNTAs since bundling can lead to intertube contacts. With intertube contacts, there is lateral charge transport between the NTs and the transport pathway is longer with a 3D conducting pathway.[27] As a result, the solar conversion efficiency is lower for TNTAs with clusters of bundling as compared with TNTAs that are independently vertically standing on the substrates.

Near-perfect ordered and densely packed TNTAs fabricated from highly ordered SFIL-based PAA templates are shown in Fig. 3A and 3B. Ordered nanoindentations are created on the Al surface to guide the growth of the ordered PAA template during anodization. The ordered nanoporous templates are in wafer sizes and can be tailored for industrial scale mass fabrication. The growth of ordered and uniform TNTAs on the ordered template is achieved by the
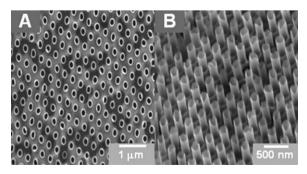

Fig. 3 Top view (A) and cross-sectional view (B) of SEM images show near-perfect ordered and densely packed TNTAs prepared by a highly ordered PAA template from a step and flash imprint lithography (SFIL)-based method. The TNTAs are of a diameter of 100 nm, height of 300 nm, interpore spacing of 300 nm and wall-thickness of 15 nm.

conformal and precise film thickness coating of the ALD technique. These near-perfect ordered TNTAs are of a diameter of 100 nm, height of 300 nm, interpore spacing of 300 nm and wall-thickness of 15 nm. The dimensions such as diameter, height and interpore spacing are well-controlled by the anodization conditions, and the wall-thickness is precisely controlled by the ALD technique. Such intrinsic properties of the highly ordered structure can lead to an enhanced electron lifetime of DSSCs due to improved charge separation and transport.

The increase in surface area of the donor–acceptor interface through morphological change in the TNTAs can be realized by employing a multi-tiered branched 3D PAA template on ITO glass substrates. Fig. 4 shows the multi-tiered branched 3D TNTAs synthesized from the 3D PAA template. Fig. 4A and 4B show the top and cross-sectional views of two-tiered branched TNTAs on ITO substrate, respectively. It can be clearly seen that the second-tier nanotubes branch out from the preceding nanotube tier. The first tier has a diameter of 270 nm, branching into four sub-pores of 110 nm in the second tier. Similarly, Fig. 4C and 4D show the top and cross-sectional views of three-tiered branched TNTAs. The first tier has a diameter of 270 nm, branching into four sub-pores of 110 nm in the second tier, and are further branched into another four sub-pores of 40 nm in the third tier. The wall-thickness is 15 nm and height is 3 μm for all branched TNTAs. These 3D multi-tiered branched TNTAs exhibit an increase in the absorptive surface area when compared with 1D single branched TNTAs. As such, we can expect a substantial increase in dye loading of the material which can enhance the solar cell efficiency.

Complete wetting and filling of TNTA-based DSSCs with dye and hole-conducting material are critical factors for the solar efficiency. We have qualitatively characterized the pore filling of TNTAs
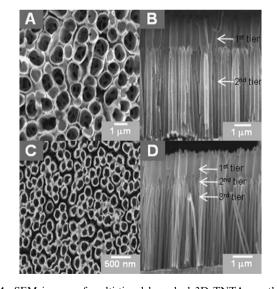
fabricated by our PAA template-assisted ALD method using cross-section SEM as shown in Fig. 5A and 5B. The TNTAs were first sensitized by immersion in 0.5 mM D102 dye overnight at room temperature and spin coated with 18 wt.% of hole-conductor solution 2,2′,7,7′-tetrakis-(N,N-di-p-methoxyphenyl-amine)9,9′spiro-bifluorene (spiro-OMeTAD). As shown in Fig. 5A, the bundling of TNTAs limits the infiltration of the dye and hole-conducting material as the nanotubes are not "wetted" by the dye and hole-conducting materials. In contrast, Fig. 5B shows that the dye and hole-conducting materials penetrated well into the pores of vertically standing TNTAs as indicated by the "wetted" region on the image. These observations were further verified and quantified by energy dispersive X-ray (EDX) spectra as shown in Fig. 6A and 6B (wt.% and at.% data in ESI†). The carbon peak in the EDX spectra is from both the dye and hole-conductor molecules which infiltrated in the TNTAs. The TNTAs bundled together on the substrates (Fig. 6A) show a lower carbon signal at an atomic weight fraction of 4%, as compared to the TNTAs that are vertically aligned on substrates at an atomic weight fraction of 16% (Fig. 6B). This pore filling fraction of TNTAs by dye and hole-conductor materials has a dominant influence on the solar cell performance.

In summary, we have demonstrated an ALD-based technique for the fabrication of vertically standing, highly ordered, and dimension and morphology controllable TNTAs on substrates via various types of PAA templates. Vertically standing TNTAs were dried by CO_2
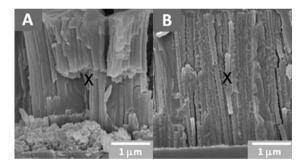

Fig. 5 Cross-sectional SEM views of TNTAs infiltrated with dye and hole-conductor materials. (A) TNTAs that have bundled together on the substrates are not infiltrated by dye and hole-conductor materials. (B) TNTAs that are vertically standing on substrates are infiltrated by dye and hole-conductor materials. The walls of the tubes can be seen to be coated with a layer of solution. Location marked "X", where EDX data, with a spot size of 0.5 μm, were taken.

Fig. 4 SEM images of multi-tiered branched 3D TNTAs synthesized from 3D PAA templates. Top view (A) and cross-sectional (B) view of two-tiered branched TNTAs, with the first tier having a diameter of 270 nm, branching into four sub-pores of 110 nm in the second tier. Top view (C) and cross-sectional (D) view of three-tiered branched TNTAs, with the first tier having a diameter of 270 nm, branching into four sub-pores of 110 nm in the second tier and further branching into another four sub-pores of 40 nm in the third tier. The wall-thickness is 15 nm and height is 3 μm for all branched TNTAs.
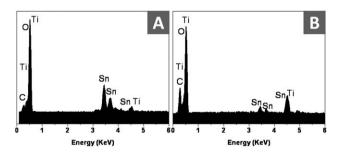

Fig. 6 Energy dispersive X-ray analysis of TNTAs infiltrated with dye and hole-conductor materials. (A) TNTAs that have bundled together on the substrates have a lower carbon element content than (B) TNTAs that are vertically standing on the substrates.

critical point drying and highly ordered TNTAs were prepared by using near-perfect PAA templates obtained *via* SFIL method. The TNTAs with controlled dimension, and morphology were prepared from 1D and 3D branched multi-tiered PAA templates. The infiltration of dye (D102) and hole-conducting material (spiro-OMe-TAD) into the prepared TNTA-based DSSCs were qualitatively and quantitatively characterized. Our approach may enable the development of novel TNTA-based solid-state dye-sensitized solar cells with improved performance. The TNTAs also provide a promising material platform that can be functionalized with upconversion nanoparticles for efficient energy harvesting.[28]

Acknowledgements

References

1 K. H. Yu and J. H. Chen, *Nanoscale Res. Lett.*, 2009, **4**, 1.
2 J. M. Macak, H. Tsuchiya, A. Ghicov and P. Schmuki, *Electrochem. Commun.*, 2005, **7**, 1133.
3 N. Q. Wu, J. Wang, D. Tafen, H. Wang, J. G. Zheng, J. P. Lewis, X. G. Liu, S. S. Leonard and A. Manivannan, *J. Am. Chem. Soc.*, 2010, **132**, 6679.
4 S. Q. Li, G. M. Zhang, D. Z. Guo, L. G. Yu and W. Zhang, *J. Phys. Chem. C*, 2009, **113**, 12759.
5 D. Gong, C. A. Grimes, O. K. Varghese, W. Hu, R. S. Singh, Z. Chen and E. C. Dickey, *J. Mater. Res.*, 2001, **16**, 3331.
6 D. Kim, A. Ghicov and P. Schmuki, *Electrochem. Commun.*, 2008, **10**, 1835.
7 P. Roy, S. P. Albu and P. Schmuki, *Electrochem. Commun.*, 2010, **12**, 949.
8 D. A. Wang, B. Yu, C. W. Wang, F. Zhou and W. M. Liu, *Adv. Mater.*, 2009, **21**, 1964.
9 K. Zhu, T. B. Vinzant, N. R. Neale and A. J. Frank, *Nano Lett.*, 2007, **7**, 3739.
10 A. Ghicov, S. P. Albu, R. Hahn, D. Kim, T. Stergiopoulos, J. Kunze, C. A. Schiller, P. Falaras and P. Schmuki, *Chem.–Asian J.*, 2009, **4**, 520.
11 T. S. Kang, A. P. Smith, B. E. Taylor and M. F. Durstock, *Nano Lett.*, 2009, **9**, 601.
12 D. Kim, A. Ghicov, S. P. Albu and P. Schmuki, *J. Am. Chem. Soc.*, 2008, **130**, 16454.
13 D. Kuang, Jérémie Brillet, P. Chen, M. Takata, S. Uchida, H. Miura, K. Sumioka, S. Zakeeruddin and M. Grätzel, *ACS Nano*, 2008, **2**, 1113.
14 L. D. Sun, S. Zhang, X. W. Sun and X. D. He, *J. Nanosci. Nanotechnol.*, 2010, **10**, 4551.
15 D. A. Wang, Y. Liu, B. Yu, F. Zhou and W. M. Liu, *Chem. Mater.*, 2009, **21**, 1198.
16 W. Zhu, X. Liu, H. Q. Liu, D. L. Tong, J. Y. Yang and J. Y. Peng, *J. Am. Chem. Soc.*, 2010, **132**, 12619.
17 O. K. Varghese, M. Paulose and C. A. Grimes, *Nat. Nanotechnol.*, 2009, **4**, 592.
18 T. S. Kustandi, W. W. Loh, H. Gao and H. Y. Low, *ACS Nano*, 2010, **4**, 2561.
19 A. Y. Y. Ho, H. Gao, Y. C. Lam and I. Rodriguez, *Adv. Funct. Mater.*, 2008, **18**, 2057.
20 M. Knez, K. Niesch and L. Niinisto, *Adv. Mater.*, 2007, **19**, 3425.
21 L. K. Tan, A. S. M. Chong, X. S. E. Tang and H. Gao, *J. Phys. Chem. C*, 2007, **111**, 4964.
22 Y. J. Lin, S. Zhou, X. H. Liu, S. Sheehan and D. W. Wang, *J. Am. Chem. Soc.*, 2009, **131**, 2772.
23 Y. J. Hwang, A. Boukai and P. D. Yang, *Nano Lett.*, 2009, **9**, 410.
24 L. Schmidt-Mende, U. Bach, R. Humphry-Baker, T. Horiuchi, H. Miura, S. Ito, S. Uchida and M. Gratzel, *Adv. Mater.*, 2005, **17**, 813.
25 I. K. Ding, N. Tetreault, J. Brillet, B. E. Hardin, E. H. Smith, S. J. Rosenthal, F. Sauvage, M. Gratzel and M. D. McGehee, *Adv. Funct. Mater.*, 2009, **19**, 2431.
26 L. Schmidt-Mende and M. Gratzel, *Thin Solid Films*, 2006, **500**, 296.
27 P. Roy, D. Kim, K. Lee, E. Spiecker and P. Schmuki, *Nanoscale*, 2010, **2**, 45.
28 F. Wang, Y. Han, C. S. Lim, Y. Lu, J. Wang, J. Xu, H. Chen, C. Zhang, M. Hong and X. Liu, *Nature*, 2010, **463**, 1061.

This journal is © The Royal Society of Chemistry 2011

J. Mater. Chem., 2011, **21**, 11084–11087 | 11087